MATEC Web of Conferences **135**, 00077 (2017) DOI: 10.1051/matecconf/201713500077
ICME'17

The effect of white etching layer patches on a larger rail defect

Shahmir Hayyan Sanusi[1,*], and *David* Fletcher[2]

[1]Department of Mechanical Engineering, Universiti Tun Hussein Onn Malaysia, Parit Raja, 86400 Batu Pahat, Johor, Malaysia
[2]Department of Mechanical Engineering, University of Sheffield, S1 3JD Sheffield, UK

Abstract. Manufacturing defects such as porosity that formed in the rail could result in catastrophic failure if it remain in service. In this study, a crack that initiated from a large void was modelled using boundary element model to investigate the effect of white etching layer patches on larger defects in rail. The configuration studied represents a large defect in the rail that was observed from a rail removed from service. These investigation has provided a better understanding of how a crack initiated from a larger defect grows under the effect of white etching layer. The results highlight that a continuous white etching layer region will dominates the growth of the crack compared to a patches white etching layer region for a smaller crack size while patches of white etching layer will accelerates the crack growth for a larger crack size. The crack growth predicted in this study for a small crack size is at least 6 times higher than the wear rate mentioned in the literature and will increase further if the expansion of a transformed layer is considered making it impossible to be removed by natural wear.

1 Introduction

Porosity, voids, and inclusions are undesirable imperfections that developed in a metal casting process. The term porosity is widely used to describe any hole or void formed in a cast product [1]. In the rail manufacturing process, porosity could be formed in rails due to improper control during the vacuum degassing process. As the molten steel changes state from liquid to solid during the manufacturing process, trapped gas that is dissolved in the molten steel would remain in bubble form as the steel solidifies [2] which could result in sudden rail fracture. Due to a greater demand in the rail transport industry, the increase in train capacity, larger axle loads, and higher speed have resulted in a greater variety and frequency on the formation of rail defects across the rail network [3]. Smaller defects may remain in track until evidence of their growth led to rail removal, but for larger defects, immediate rail replacement is required [4].

* Corresponding author: shahmir@uthm.edu.my

Numerous studies has been done in the past to investigate the effect of inclusions in rails [5]–[10]. If inclusions remain in the rail, they may establish a favoured region of stress concentration. Potential damage process might develop (depending on the level of stress and wear rate) which could result in catastrophic failure. Observation from recent work [11] suggests that the metallurgical transformed regions sometimes form as patches (not continuous) with various length and thickness. Therefore it would be interesting to study the effect of this transformed region on cracks that initiated from larger defect in rail. To demonstrate these issues, a simple two dimensional (2D) boundary element (BE) model was developed within the Beasy software package [12] to investigate the influence of patches white etching layer region (Figure 1) on a larger defect in rail.

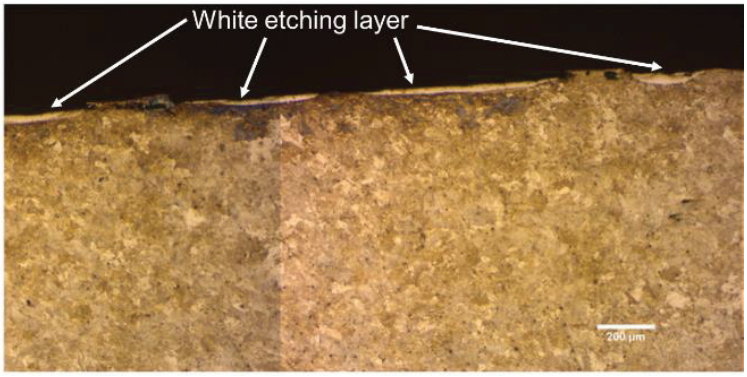

Fig. 1. Patches of white etching layer lying on the rail surface

2 Modelling method and conditions

A specific defect (Figure 2) described in the morphological study [11] is considered in the modelling. The model variables and conditions were decided to match the operating condition of a high speed traffic. An in-depth case study is made of a large void (maximum length of 2.9 mm and a maximum height of 0.9 mm) that was modelled to investigate the effect of white etching layer patches on a larger defect in rail. The defect was located approximately 2 mm below the rail surface with two inclined cracks (referred as left and right crack) initiated from the left and right side of the void. The left crack has an inclination angle of 4.65° while the right crack has an inclination angle of 15.68°. Different crack lengths (0.5 mm, 1 mm, 2 mm, and 4 mm) were considered to examine the crack growth rate. The real geometry of the defect was modelled by extracting the defect perimeter coordinates from the metallographic image using an open source data extractor package known as the G3data [13].

Fig. 2. Example of massive void morphologhy below the running band in a longitudinal cross section from a high speed mixed traffic line. The central portion of the defect lies approximately 2 mm below the rail surface. Incline crack initiated from the left and right side of the void. The white marker above the rail surface indicates the location of a patch of white etching layer with a thickness ranging between 20 to 250 µm.

Table 1. Conditions modelled.

Case	Consideration
1	No metallurgical transformed layer
2	Continuous thin (0.25 mm) metallurgical transformed layer (length: 4 mm)
3	Patches of thin (0.25 mm) metallurgical transformed layer (length: 6 mm)

Three cases have been considered throughout this study as indicated in Table 1. For case 1, no metallurgical expansion layer has been considered and case 1 has been chosen as the baseline case to identify the effect when a metallurgical transformed layer with a different configuration exist above the larger defect. The configuration of the model for case 1 is shown in Figure 3a. For case 2, a thin metallurgical transform layer with a thickness of 250 µm lying above the defect was considered where the total length of the transform region was set to be 4 mm covering the whole length of the void (Figure 3b). Case 3 represents patches of metallurgically transformed region where two additional transform regions with a length of 1 mm were placed on the left and right side of the main transform region with a spacing of 1 mm between the additional transform region and the main transform region (Figure 3c). The white etching layer was represented in the model by applying a thermal body load to the whole region of transformed layer which symbolizes an expansion of a surface layer due to volume change. The value of expansion due to transformation was taken as 0.8% which was calculated based on the changes in density from pearlite to martensite as described in [14].

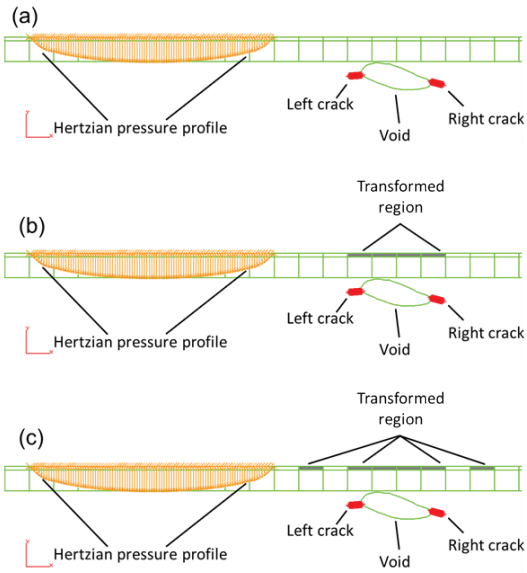

Fig. 3. Representation of BE model of rail–wheel contact for 2 incline cracks initiated from the left and right side of a larger defect (named as left and right crack). (a) case 1 - no metallurgical transform region considered. (b) case 2 – thin metallurgical transform region lying above the void with a continuous length of 4 mm and a thickness of 250 µm. (c) case 3 – similar with case 2 where thin metallurgical transform region lying above the void with a continuous length of 4 mm and a thickness of 250 µm. Two additional transform region with similar thickness and a length of 1 mm was placed on the left and right side of the main transformed region with a spacing of 1 mm to represent patches of transformed region.

3 Results and discussions

All the cases listed in Table 1 were investigated for a 0.5 mm crack length to examine a crack that has initiated from a void but not yet grown significantly. Modelling was also performed for a range of crack lengths of 1 to 4 mm to investigate the effect of a different configuration of the metallurgical transformed layer on propagated cracks. For each condition modelled, the range of stress intensity factor was assessed by considering the movement of a wheel incrementally across the defect (Figure 4), generating a series of SIFs. The combined action of traction and normal stress is indicated in the figure, and results in asymmetry of the results for left and right crack tips. Results are presented as stress intensity factors in Figure 5 to Figure 7, in which the origin is at the void centre. Stress intensity factors are converted to indicative crack growth rates as display in Figure 8.

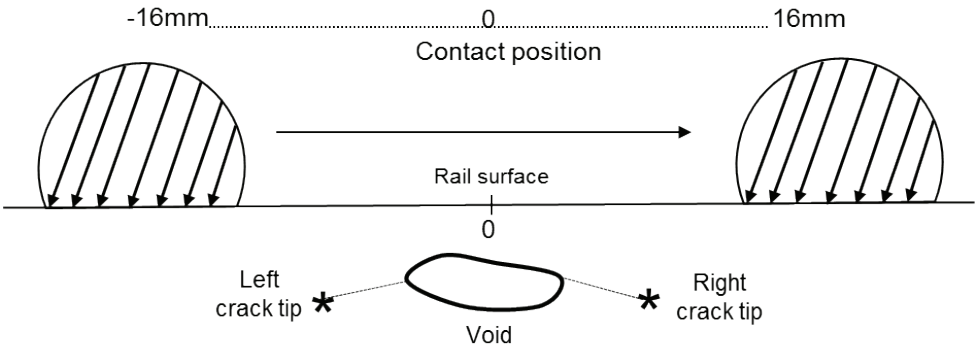

Fig. 4. A series of analyses are performed with incremental movement of the contact across the defect. The origin of the position is measured from the centre of the void.

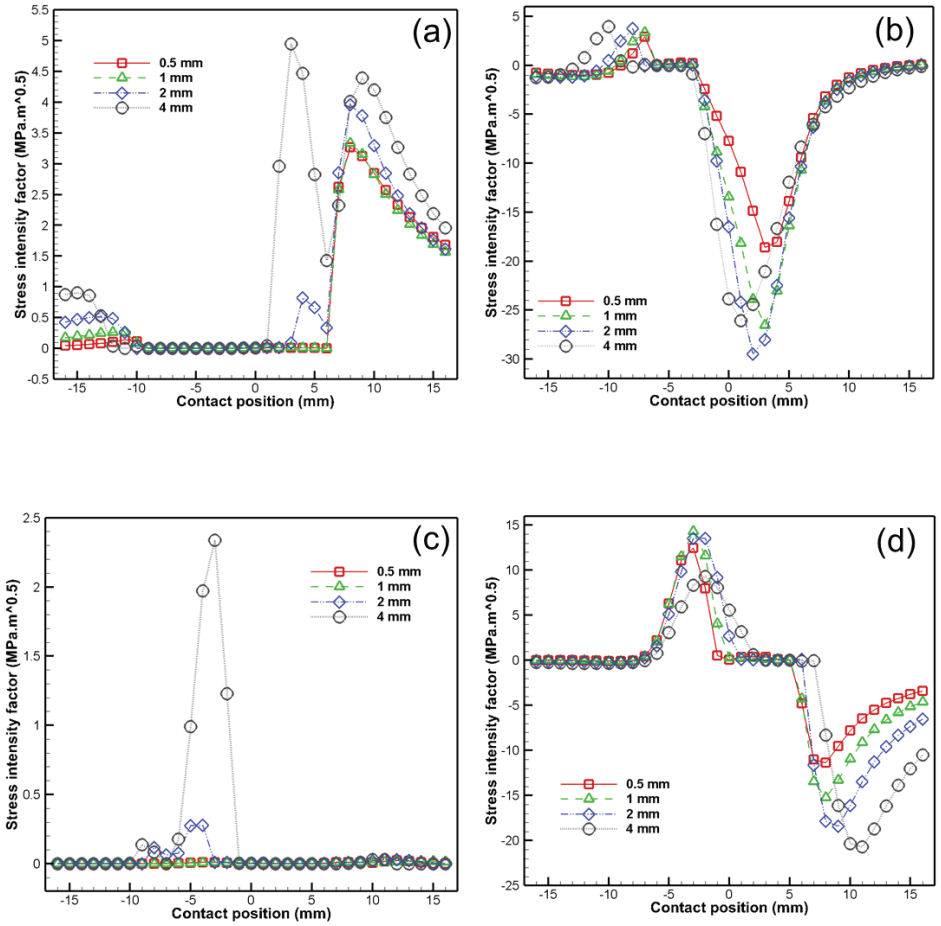

Fig. 5. Stress intensity factor dependence on contact position. (a) left tip mode I, (b) left tip mode II, (c) right tip mode I, and (d) right tip mode II

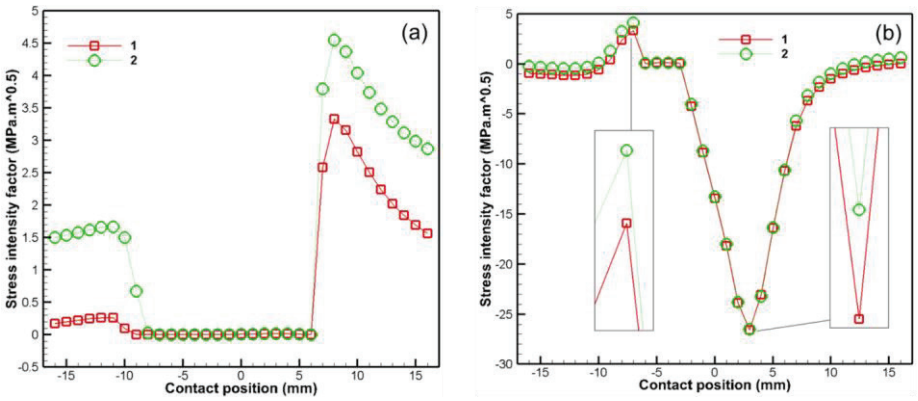

Fig. 6. Effect of a thin metallurgical expansion layer (represented as density change) on stress intensity factor for 1 mm crack, left crack tip. (a) Mode I, and (b) mode II. Legend entries refer to cases in Table 1.

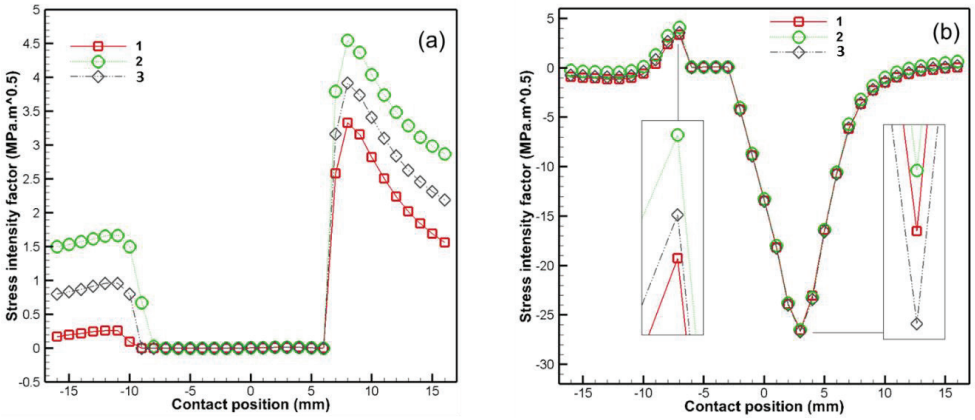

Fig. 7. Effect of thin metallurgical expansion layer patches (represented as density change) on stress intensity factor for 1 mm crack, left crack tip. (a) Mode I, and (b) mode II. Legend entries refer to cases in Table 1.

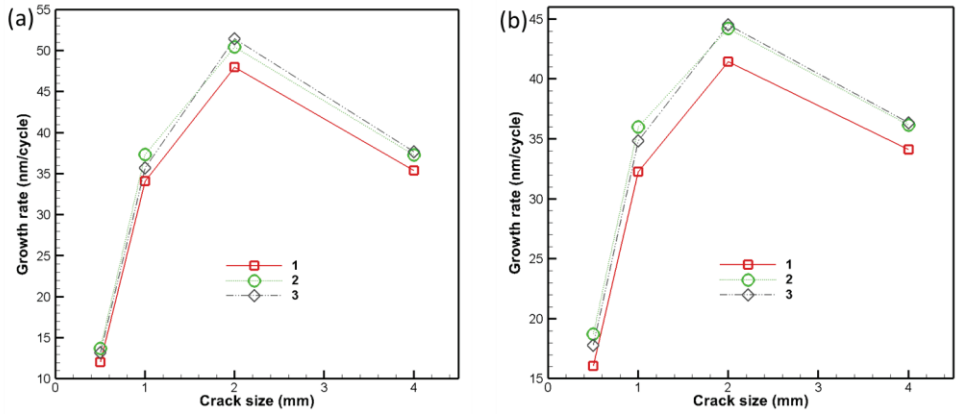

Fig. 8. Crack growth rate dependence on crack size for all cases considered. (a) Left crack tip, and (b) right crack tip. Legend entries refer to cases in Table 1.

3.1 Stress intensity factor dependence on crack size

The trends in mode I and mode II SIF for the left and right crack tips that initiated from a larger defect is shown in Figure 5 where consideration was made for case 1. This case only considered mechanical load (without considering any metallurgical transformed layer above the void). The mode I SIF shows a rise with increasing crack size for the left crack tip (Figure 5a), but the values are small even for larger cracks (4mm) where the peak KI is still below the threshold SIF (6 MPa.m1/2 for tensile growth of cracks in carbon steel [15]). Data for the mode II SIF (Figure 5b) shows higher stress intensity factor values even for smallest crack where the range exceeded the shear mode threshold of 1.5 MPa.m1/2 proposed by Otsuka et al. [15]. Even though the value of mode I SIF does not exceed the opening mode threshold, crack growth would still be expected since the range of mode II SIF exceeded the shear mode threshold value.

For the right crack tip, the range of KI and KII show rising trends with increasing crack size (Figure 5c and d). However, there was some reduction in the range of KII once the

crack reaches a size of 4 mm for the left and right crack tip. This reflects the trend in the outcome of crack growth under mixed mode developed for inclined surface breaking cracks (Figure 8 and Table 2) where there is an increase in the growth with an increase of crack size, but decreased once both cracks exceeded a size of 2 mm.

Table 2. Crack growth rates (nm/cycle) for all the cases and sizes of crack modelled.

Case	0.5 mm		1 mm		2 mm		4 mm	
	L	R	L	R	L	R	L	R
1	12.0	16.0	34.1	32.3	48.0	41.5	35.4	34.1
2	13.7	18.7	37.3	36.0	50.4	44.2	37.3	36.1
3	13.2	17.8	35.7	34.9	51.4	44.5	37.7	36.3

As the crack size increase, the tip moves deeper into the material where the stress region become lesser with an increasing depth. A similar observation can be seen from the shear stress plot (Figure 9) where the magnitude of the shear stress starts to decrease with an increasing depth. As the crack reach some critical crack length and depth, this results in a reduction in stress intensity value hence resulting in a drop in the growth rate [16]. Therefore, the propagation of the crack may tend to slow even though the crack elongate. Place the figure as close as possible after the point where it is first referenced in the text. If there is a large number of figures and tables it might be necessary to place some before their text citation.

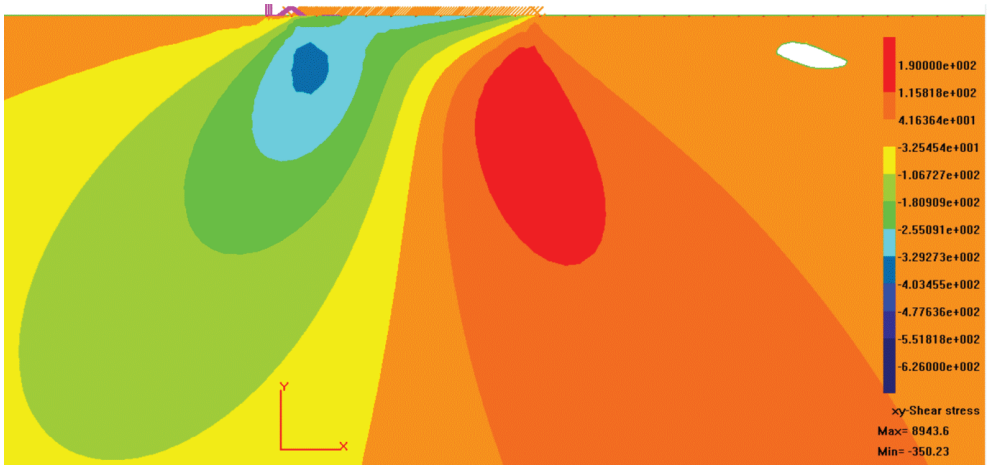

Fig. 9. Shear stress plot at -16mm contact (far away from the defect) for case 1. Units in MPa

3.2 Expansion effect of a thin surface layer on cracks initiated from void

The effect of the thin expansion layer on mode I and II SIF for the left crack tip is shown in Figure 6 and the baseline (case 1) is included for comparison. The trend (Figure 6a) shows that the presence of the metallurgical transformed layer has a significant effect on the mode I SIF where its value will always be above the baseline case if the contact is far from the crack tip. However, this effect is only valid for short crack size (0.5 – 2 mm) whereby for the largest crack (4 mm), the expansion of the transformed layer gives very minor effect on

the KI value. This phenomenon is similar to the case for horizontal crack [14] where the effect will diminish as the crack lengthens. Even though the expansion of the transformed layer give a rise on the KI value, the range is still below the opening tensile threshold even for the largest crack size. For mode II data (Figure 6b), the trend shows that the expansion of the transformed layer increases the magnitude of the negative and positive peak but the effect is small. These differences can be seen numerically in Table 3. The changes are small and reduce as the crack extends. Results for the right crack tip exhibit similar behaviour where expansion of the transformed layer only affects the range of KI value for shorter crack and gives very little effect on the range of mode II SIF.

Table 3. Mode I and Mode II SIF range for all case modelled.

Case	0.5 mm				1 mm				2 mm				4 mm			
	L		R		L		R		L		R		L		R	
	ΔK_I	ΔK_{II}	ΔK_I	ΔK_{II}	ΔK_I	ΔK_{II}	ΔK_I	ΔK_{II}	ΔK_I	ΔK_{II}	ΔK_I	ΔK_{II}	ΔK_I	ΔK_{II}	ΔK_I	ΔK_{II}
1	3	21	0	23	3	29	0	29	4	33	0	32	4	30	2	30
2	4	22	1	24	4	30	1	30	4	33	1	32	4	30	2	30
3	4	22	1	24	3	30	1	30	4	33	1	32	4	30	2	30

The expansion of the metallurgical transform layer lying above the defect will introduce an opening stress region below its whole length until a certain depth as shown in Figure 10. It can be seen that the region of the maximum opening stress occured at the side of the defect where crack initiation point is located. For the shortest crack (0.5 mm), the whole length of the crack is situated at the region where maximum opening stress occured (e.g. y-direction direct stress). As the crack lengthens, the crack tip had exceeded these maximum stress regions where only some part of the crack length is affected by the opening stress and this will result in a very minor reduction in the KI value as the crack lengthens.

Fig. 10. Deform vertical stress plot for the case where thin expansion layer is present above the defect (case 2). Mechanical load (contact) and crack were absent. The deformation plot scale factor was set to 100 for clarity. Units in MPa.

3.3 Effect of patchy transform region

The effect of a patchy transformed region on mode I and mode II SIF for 1 mm crack focusing on the left crack tip can be seen from Figure 7. The trend in Figure 7a shows that the value of KI rises above baseline (case 1) but fall below case 2 throughout all positions of the contact. Looking at the numerical changes in Table 3, the trend change where the range of mode I SIF for case 3 raise above ΔKI for case 2 as the crack lengthens from 2 mm to 4 mm. Although the SIF changes are small, they do influence the trend of the crack growth (Figure 8) where patches of white etching layer will drive to a higher crack growth in case 3 compared to case 2 as the crack lengthens. For the mode II data (Figure 7b), the patches of the transform region give minimal but variable effect on the range of mode II SIF. For all sizes of crack modelled, it was found that patchy white etching layer has an insignificant effect on the ΔKII value compared to case 2.

Looking at the results overall, when patches of transform region formed on the surface, they will introduce an opening stress region below the transformed region (similar to case 2) due to volume expansion. However, the presence of gap/spacing between the transform region will introduce an additional compressive stress region below the gap (Figure 11). Since the transform region expands due to volume expansion particularly noticeably when the contact is not present, the non-transformed region of the gap will compress due to the reaction movement (Newton 3rd law) and this will result in the formation of the compressive stress region under the gap. Therefore any crack tip that lies in this region will experience compressive stress that will reduce its KI value. Focusing on the left crack tip, Figure 12 show the deformed plot for case 3 when the contact is not present. For the 1 mm crack size, some part of the crack is located at the tensile stress region while some part especially the crack tip is located at the compressive stress region (Figure 12a). This results in a small reduction in the ΔKI value compared to case 2 for similar crack size. However, as the crack lengthens to a size of 2 mm, some part of the crack especially near the crack tip is located at the opening stress region (Figure 12b) and this attribute to higher ΔKI value compared to case 2. Hence although minor, the variation in SIF observed can be seen to be caused by the physical region modelled and not by artifacts of the modelling process.

Fig. 11. Deform vertical stress plot for the case where patches of thin expansion layer are present above the defect (case 3). Mechanical load (contact) and crack were absent. The deformation plot scale factor was set to 100 for clarity. Units in MPa.

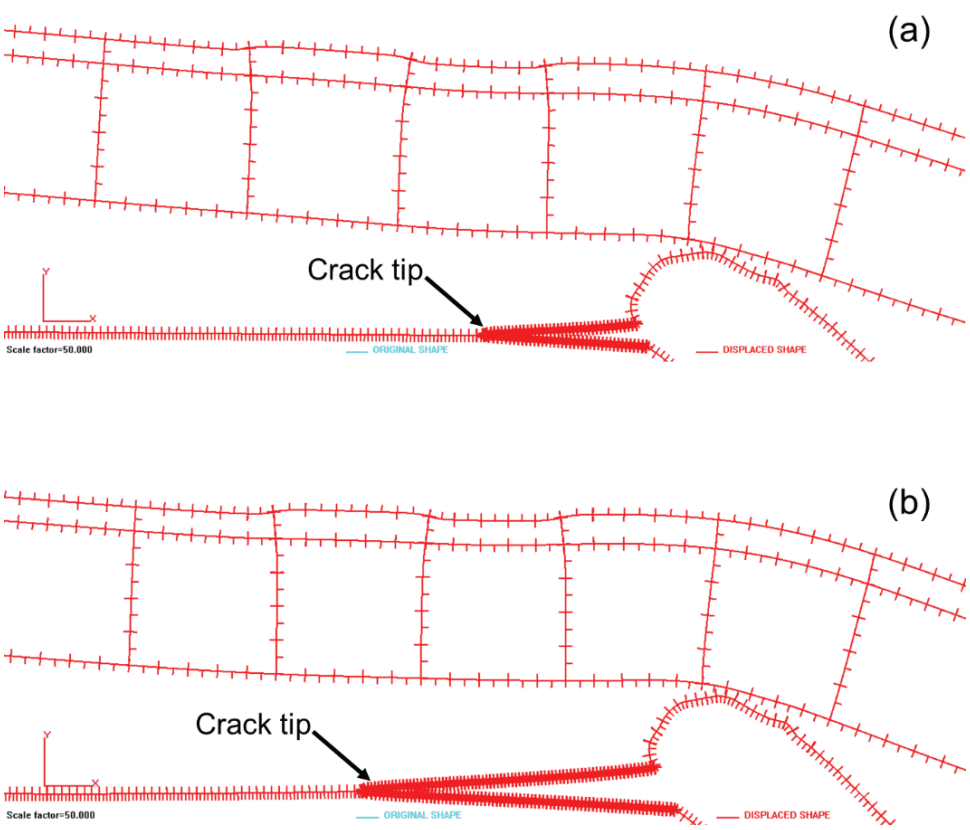

Fig. 12. Deformed plot for the case where patches of thin expansion layer are present above the defect (case 3) focusing on the left crack tip. Mechanical loads (contact) were absent. The deformation plot scale factor was set to 50 for clarity. (a) 1 mm crack size. (b) 2 mm crack size.

3.3 Real world consideration

It is known that there is an interaction between wear and fatigue crack whereby some rail steel grades wear more rapidly, and small cracks are always removed when wear process dominates. Typical rail wear rate measured from twin disc test under a dry condition with a maximum pressure of 1500 MPa is around 1.05 nm/cycle [17] where the value would rise up to 2.5 nm/cycle when decarburised layer are present on the rail surface [18]. However the crack growth predicted in this study for a small crack size is at least 6 times higher than the wear rate mentioned in the literature, and its growth rate will rise if the expansion of a transformed layer is considered.

4 Conclusions

Severe thermal loading for example caused by poor traction control has resulted in a formation of a thick metallurgical transformed layer on the rail surface which is known as the white etching layer. The presence of white etching layer on a rail remove from service (normally associated with squat type defect) comes in various type of form where sometimes the layer is not continuous and appear in the form of patches with various

thickness and sizes. The effect of different WEL configurations on an inclined crack initiated from larger defect have been studied leading to the following conclusions:

a) The presence of thin (0.25 mm) metallurgical transformed layer / white etching layer lying above the defect will give an increase in the growth rate for an inclined crack. However, the effect reduces with an increasing crack size as the crack tip moves away from the region of maximum stress.

b) Patches of white etching layer will have lower crack growth compared to a continuously transformed layer while the crack tip is below region which is not transformed. However, the rate will increase once the crack tip enters the next region of a following metallurgical transform layer.

Since the crack considered in the model is subsurface, therefore there is no interaction of the crack and wear. But to give some context to its growth rate, it was found that the growth rate is at least 6 times higher than the wear rate mentioned in the literature, and its growth rate will rise if the expansion of a transformed layer is considered. Looking at the overall behaviour of the crack (Figure 2), there is a tendency for this crack to grow transversely potentially leading to rail fracture under bending stress. Therefore, immediate rail replacement is required once the crack grows to its critical crack length [17].

References

1. AFS, "Understanding Porosity," American Foundary Society, 2016. [Online]. Available: http://www.afsinc.org/content.cfm?ItemNumber=6933. [Accessed: 17-Oct-2016].
2. R. D. Pehlke, "Formation of Porosity During Solidification of Cast Metals," in Foundry Processes: Their Chemistry and Physics, S. Katz and C. F. Landefeld, Eds. Boston, MA: Springer US, 1988, pp. 427–445.
3. S. Kumar, S. Gupta, B. Ghodrati, and U. Kumar, "An approach for risk assesment of rail defects," Int. J. Reliab. Qual. Saf. Eng., vol. 17, no. 4, pp. 291–311, 2010.
4. D. F. Cannon, K. O. Edel, S. L. Grassie, and K. Sawley, "Rail defects: An overview," Fatigue Fract. Eng. Mater. Struct., vol. 26, no. 10, pp. 865–886, 2003.
5. H. K. Jun, J. W. Seo, I. S. Jeon, S. H. Lee, and Y. S. Chang, "Fracture and fatigue crack growth analyses on a weld-repaired railway rail," *Eng. Fail. Anal.*, vol. 59, pp. 478–492, 2016.
6. D. M. Fegredo, M. T. Shehata, A. Palmer, and J. Kalousek, "The effect of sulphide and oxide inclusions on the wear rates of a standard C-Mn and a Cr-Mo alloy rail steel," *Wear*, vol. 126, no. 3, pp. 285–306, 1988.
7. Z. Mouallif, B. Radi, and I. Mouallif, "The thermomechanical modeling of aluminothermic welds affected by different defects Summary :," *Int. J. Eng. Res. Develoment*, vol. 11, no. 10, pp. 44–48, 2015.
8. Z. Mouallif, B. Radi, and I. Mouallif, "Effect of the Inclusion Defect on the Mechanical Behavior of Thermite Welds," *Adv. Theor. Appl. Mech.*, vol. 9, no. 1, pp. 11–20, 2016.
9. I. Mouallif, Z. Mouallif, A. Benali, and F. Sidki, "Finite element modeling of the aluminothermic welding with internal defects and experimental analysis," in *MATEC Web of Conferences*, 2012, vol. 1, p. 12.
10. J. E. Garnham, R.-G. Ding, and C. L. Davis, "Ductile inclusions in rail, subject to compressive rolling–sliding contact," *Wear*, vol. 269, no. 11–12, pp. 733–746, Oct. 2010.
11. D. I. Fletcher and S. H. Sanusi, "SBB Rail Analysis," Sheffield, 2013.

12. "BEASY Boundary Element software." [Online]. Available: www.beasy.com. [Accessed: 04-Aug-2016].
13. G3data, "G3data," 2010. [Online]. Available: https://github.com/pn2200/g3data.
14. D. I. Fletcher and S. H. Sanusi, "The potential for suppressing rail defect growth through tailoring rail thermo-mechanical properties," *Wear*, 2015.
15. A. Otsuka, K. Mori, and T. Miyata, "The condition of fatigue crack growth in mixed mode condition," *Eng. Fract. Mech.*, vol. 7, no. 3, pp. 429–439, Sep. 1975.
16. A. Kapoor, D. I. Fletcher, and F. J. Franklin, "The role of wear in enhancing rail life," *Tribol. Res. Des. Eng. Syst. Proc. 29th Leeds-Lyon Symp. Tribol.*, vol. Volume 41, no. 0, pp. 331–340, 2003.
17. "Rolling contact fatigue in rails: a guide to current understanding and practice," in *RT/PWG/001 Issue 1*, Railtrack PLC, 2001, p. 46.